Turk J Chem
34 (2010) , 815 – 824.

doi:10.3906/kim-0908-176

Electrochemical impedance spectroscopic studies of the passive layer on the surface of copper as a function of potential

Amtul NASEER[1,*], **Athar Yaseen KHAN**[2]
[1] *Chemistry Department, Quaid-i-Azam University, Islamabad-PAKISTAN*
[2] *Chemistry Department, Allama Iqbal Open University, H-8, Islamabad-PAKISTAN*
e-mail: hanm_7@yahoo.com

Received 06.08.2009

Electrochemical impedance spectroscopy (EIS) and cyclic voltammetry (CV) were used to investigate the oxide layer formed on a copper disc electrode and the changes that took place when treated potentiostatically in the range of -0.3 V to 0.9 V in buffer of pH 8.5. The response of an electrode using EIS, initially at equilibrium, to an applied potential was then modeled with equivalent circuits, proposed for different potential regions that completely illustrated the Cu/oxide/electrolyte systems and their properties in terms of 2 interfaces. Criterion for the applicability of equivalent circuit models was discussed. Changes in the film/metal interface as a function of potential were also probed at 30 mHz using Nyquist plots. Diffusion coefficient and concentration of mobile ions in the film calculated from the EIS data came out of the order of 10^{-6} cm^2 s^{-1} and 10^{-6} mmol mL^{-1}, respectively.

Key Words: Copper; electrochemical impedance spectroscopy; cyclic voltammetry; passive film; interfaces

Introduction

The growth pattern of passive film formation and breakdown was investigated earlier in buffer solution of pH 9.2.[1] The passive film that formed over the copper surface mainly consisted of a barrier layer of Cu_2O and a duplex film $CuO/Cu(OH)_2$. Feng et al.[2] showed the strong reliance of film texture on the pH of the solution and since the film formation has attracted considerable interest in many areas of research to study the phenomena of corrosion, electro-catalysis and double layer structures[3] it is useful to study its anodic behavior in aqueous

*corresponding author

media of weakly acidic or alkaline pH. Nevertheless, in the past, passive layers on copper metal have been investigated with full concentration.[4–7] Recently studies in corrosion of micro and nano particles of copper[8] and pre-patinated copper[9] have also been reported.

Quite a large number of surface analytical and electrochemical tools have been used to explore the film's corrosion behavior.[10–14] In spite of all this; electrochemical impedance spectroscopy is a powerful and sensitive in situ technique to characterize the surfaces. EIS was used as the main technique in the present work to explain the mechanism responsible for the growth and degradation of passive film, mainly composed of Cu_2O and CuO/Cu(OH), under applied potential in buffer solution, pH 8.5.

Experimental

The details of the copper disc electrode construction and cleaning of its surface have previously been described.[1]

Triply distilled water was used to prepare buffer solution of pH 8.5 by mixing 0.3 M H_3BO_3 with 0.075 M $Na_2B_4O_7$ in required volumes and the hydrogen ion concentration was monitored with a Horiba pH meter (Japan). A standard 3-electrode cell was used for electrochemical measurement. The electrode was pretreated at –1.4 V for 45 s using PAR 173 potentiostat/galvanostat and the cyclic voltammogram was recorded at a scan rate of 50 mV/s in the range of –1.2 V to 1.0 V with spirally coiled platinum wire as counter electrode. All potentials in this work were in reference to the saturated calomel electrode (SCE).

Impedance data at ambient temperature in the frequency range of 30 mHz to 100 kHz were collected using a 3-electrode system, on a TFA 2000 Impedance Analyzer from Sycopel Scientific, U.K. The interfering circuit of the reference electrode was removed by connecting a platinum wire electrode serving as sonde via a 10 μF capacitor. The strength of the perturbation potential used in all measurements was 5 mV peak to peak. Prior to measurement at each potential the sample disc was potentiostatically polarized to the desired potential. The impedance data were collected after a waiting period of 10 min.

Results and discussion

CV Studies of copper surface

CV (Figure 1) of a freshly prepared copper surface recorded in solution of pH 8.5 at 50 mV s^{-1} sweep rate displayed 2 anodic and 2 cathodic peaks: A_1 due to electroformation of Cu_2O and A_2 owing to CuO formation. Moreover, a very broad shoulder over an extended potential region most probably due to $Cu(OH)_2$ was also obtained. The 2 cathodic peaks were unquestionably due to electroreduction of CuO and $Cu(OH)_2$ to Cu_2O, and Cu_2O to Cu, respectively. The total cathodic and anodic currents were almost equal. The peak resolution appeared to be dependent upon the nature of the buffer. According to Pourbaix[15] the following redox reactions were expected to take place in aqueous electrolyte at pH 8.5:

$$2Cu + H_2O = Cu_2O + 2H^+ + 2e^-; E = -0.269V/SCE \quad (1)$$

$$Cu + H_2O = CuO + 2H^+ + 2e^-; E = -0.170V/SCE \quad (2)$$

$$Cu + 2H_2O = Cu(OH)_2 + 2H^+ + 2e^-; E = -0.131V/SCE \quad (3)$$

$$Cu_2O + H_2O = 2CuO + 2H^+ + 2e^-; E = -0.071V/SCE \tag{4}$$

$$Cu_2O + 3H_2O = 2Cu(OH)_2 + 2H^+ + 2e^-; E = 0.007V/SCE \tag{5}$$

Overpotential significantly affected both the anodic and the cathodic peaks. Consequently, anodic peaks were shifted to lower and cathodic peaks to higher potentials.[3]

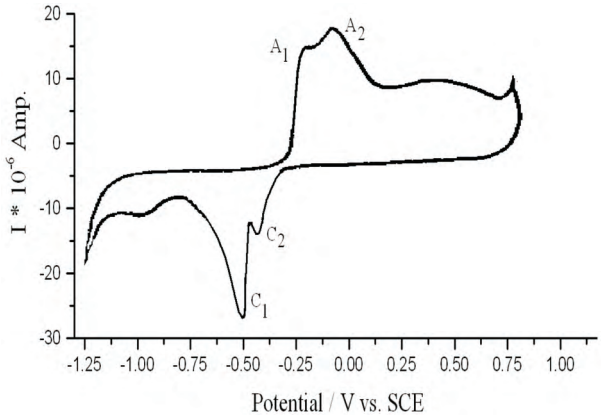

Figure 1. Cyclic voltammogram of copper in buffer solution of pH 8.5 at a scan rate of 50 mV/s.

EIS studies of copper surface

The impedance characteristics of the freshly prepared copper electrode surface as a function of frequency were studied in the 30 mHz-100 kHz range under static potential condition from –0.3 V to 0.9 V. The potential in this range was progressively increased in steps of 0.1 V. The experimental data obtained were analyzed and fitted using Electrical Equivalent Circuit (EEC) software by Boukamp.[16]

As in the case of pH 9.2,[1] 3 distinct potential regions were identified from the fitting results for the entire potential range: (a) initial stage, of oxides growth –0.3 to 0.0 V; (b) middle stage, structural changes, 0.1 to 0.3 V; and (c) final stage, transpassivity region, 0.4 to 0.9 V. Equilibrium redox potentials for the formation of Cu_2O from copper and CuO, $Cu(OH)_2$ from Cu_2O (Eqs. (1) to (5)) showed that in the first potential region the formation and growth of the inner layer of Cu_2O and the outer layer of $CuO/Cu(OH)_2$ overlaying the Cu_2O barrier layer occurred as in Figure 2. Capacitive circuit (inset Figure 3), which characterized a diffusion process, represented the behavior of the modified film. In the third potential region diffusion controlled kinetic phenomenon changed to a charge transfer process especially at 0.4 and 0.7 V.

It should be pointed out that EIS is a potentiostatic technique and, prior to EIS measurements at each potential step, the electrode was given sufficient time for stabilization.

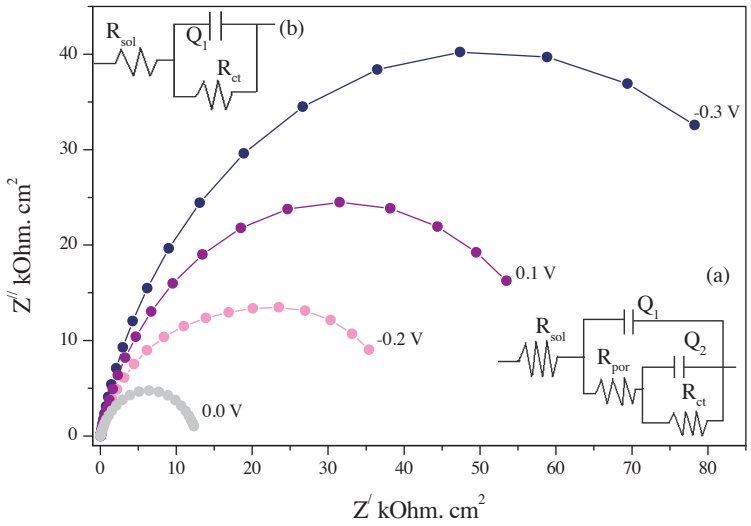

Figure 2. Nyquist plots for the initial stage of passivation of copper surface and the circuits used to fit the impedance data.

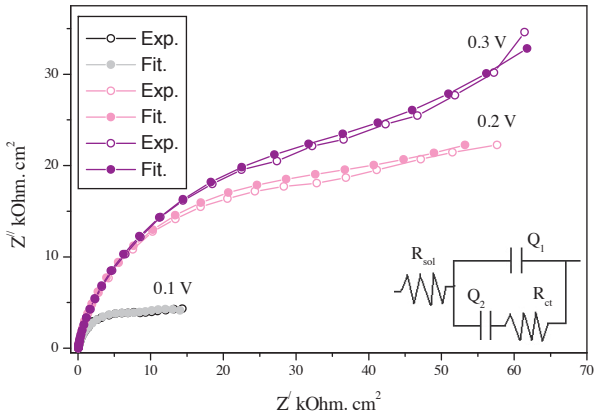

Figure 3. Experimental and fitted Nyquist plots for the second stage of passivation of copper surface and the circuit used to fit the impedance data.

Initial stage

Complex plane plots for the potentials of initial stage are shown in Figure 2. The Nyquist plotted with normalized Z′ and Z″ scale showed semicircles building up as the potential increased and completed at 0.0 V (Figure 2). The behavior of the film in relation to its continuously varying structure on application of potential is best represented by fitting the impedance data to the circuits shown in the inset (a) for –0.3 V to –0.1 V and inset (b) for 0.0 V in Figure 2. The latter was a characteristic Randle circuit for the passive layer in pH 8.5. Better agreement was achieved between theoretical and experimental results by the inclusion of frequency dependent constant-phase-elements (CPE), Q_1 and Q_2 in the circuits (Table). In general CPE appeared due to a distribution of relaxation times arising from inhomogeneities present at microscopic level in the oxide phase

and at the oxides/electrolyte interface due to a number of reasons.[17,18] The impedance of a CPE is defined by Eq. (6):

$$Z_{CPE} = [Q(j\omega)^n]^{-1} \tag{6}$$

where 1/Q is numerically equal to impedance at $\omega = 1$. For n = 1, the impedance represents the value for a true capacitance (ideal case of no dispersion); for n = 0, Z_{CPE} becomes equivalent to resistance. The value of n = 0.5 corresponds to diffusion of a reactant in a Faradaic process and Z_{CPE} represents Warburg impedance. At intermediate values 1 > n > 0.5 Eq. (6) describes the frequency behavior of a constant phase element. Magnitude of the exponent 'n' indicates the extent of surface homogeneity.

Table. EIS best fit parameters of copper surface at various potentials.

E (V vs. SCE)	$Q_1 \times 10^{-6}$ Ω^{-1} cm^{-2} s^n	n_1	R_{por} k Ω cm^2	R_{ct} k Ω cm^2	$Q_2 \times 10^{-6}$ Ω^{-1} cm^{-2} s^n	n_2
–0.3	28.0	0.85	0.20	13.6	124	0.96
–0.2	8.42	1.00	0.40	102	15.3	0.88
–0.1	27.8	0.82	0.53	64.1	17.0	0.77
0.0	27.7	0.82	-	12.66	-	-
0.1	18.6	0.87	4.65	-	148	0.25
0.2	6.88	0.90	3.62	-	25	0.21
0.3	6.19	0.89	10.5	-	24.5	0.28
0.4	27.5	0.87	1.29	14.3	429	0.60
0.5	25	0.85	6.67	36.1	86.9	0.72
0.6	25.9	0.85	3.30	44.1	32.9	0.44
0.7	33.5	0.83	2.47	10.1	33.2	0.69
0.8	147	0.85	0.09	52.2	182	0.82
0.9	312	0.77	0.18	16.6	98.6	0.90

The electrolyte/film interface is represented by Q_1 and film/metal interface by Q_2. R_{por} and R_{ct} represent film resistance and charge transfer resistance, respectively. Similarly, n_1 represents the inhomogeneity of the electrolyte/film interface and n_2 represents the inhomogeneity of the film/metal interface. The rate of corrosion was controlled by charge transfer resistance, R_{ct}. The Q_2 and R_{ct} combination characterized a higher time constant and therefore it was connected to the processes occurring at lower frequency. The Q_1 and R_{por} parallel combination characterized a lower time constant and it was connected to processes occurring at higher frequencies. It reflects the properties of oxide/electrolyte interface and refers to the double layer capacitance and resistance of electrolyte in the pores of the film.

The analysis of the impedance data was based on the criteria discussed by Walter:[19]

$$0.05 > \tau_t/\tau_p > 20 \text{ and } 0.2 < R_{ct}/R_{por} < 5 \tag{7}$$

They should be met for the experimental data to be resolved into 2 semi-circles. Generally, each time constant gave rise to a semi-circle when 2 time constants were quite far apart from each other, so that the phenomena represented by them were non-interacting and they can be effectively studied independently.

Here τ_t and τ_p stand for time constant for high frequency and low frequency, respectively. the appearance of one semicircle (incomplete) in Figure 2 indicated that the 2 time constants did not differ from each other widely as required. The diameter and the maximum reactance (Z'') at low frequencies gave R_{ct} and Q_2 strictly in accordance with the equivalent circuit model used. R_{por} and Q_1 strongly influenced the electrolyte/film interface. The shape of a wide open capacitive arc was characteristic of a capacitor charged via CPE.

R_{ct} values were always higher than R_{por} and inversely related to the exchange current density; thus they measured the corrosion rate. A higher R_{ct} value at –0.2 V indicated the presence of a Cu_2O barrier layer with some $CuO/Cu(OH)_2$ formed at later potentials (-0.1 and 0.0 V) from Cu_2O. The film appeared compact and protective. The capacitance values in this initial potential stage can be rationalized in terms of charge transfer processes leading to conversion of Cu to Cu^{1+} and Cu^{2+}, and Cu^{1+} to Cu^{2+}. A high capacitance value at –0.3 V suggested charge accumulation due to contact with electrolyte that led to a well organized Cu_2O component formed at later potentials thus completely covering the surface. The decrease in n_2 with increasing applied potential suggested that the film was losing its initial homogeneity due to reactions of Eqs. (2) to (5). This modified the circuit topology at 0.0 V.

Q_1, n_1, and R_{por} characterized the oxide film/electrolyte interface. Q_1 values first decrease and then increase. At –0.2 V, Cu_2O is formed and this aspect is reflected in the Q_1 and n_1 values.[20] With the further development of oxides at –0.1 V the interface became less homogeneous. In fact, at 0.0 V, a loose film texture is postulated. That leads to filling of pores with electrolyte and facilitated the approach of OH^- ions to the underlying surface, causing a charge transfer reaction. The passive films always possessed water in their texture, which is not free water but occurs as hydroxide or hydrated oxide or both.[21]

Middle stage

The changes in oxide film as a result of potential increase are apparent by the varying shapes of Nyquist plots as in Figure 3. The potential range for this stage extended cathodically in comparison to the potential range for the film formed in pH 9.2.[1] For 0.1 and 0.2 V a steeply rising circular arc was more distinct at high frequency. That changed to an arched line at low frequency, indicating the presence of a CPE. This shape was characteristic of a diffusion controlled process, which in this case was responsible for the movement of ions and accumulation of charge in the bulk film.

At 0.3 V, the Nyquist plot shows a circular arc at high frequency side interacting with a 'rising tail' at low frequency. The ascending part of the plot at lower frequencies is inclined at an angle of 45° to the Z' axis. The higher value of (Z', Z'') confirms a compact and rigid film by diffusion of ionic species into the duplex layer.

The proposed modified Randle circuit (Figure 3, inset) represented the diffusive character of the film. It consisted of an electrolyte/film interface denoted by Q_1 in parallel with R_{por} and another for the film/metal interface. The kinetic parameter characterizing the diffusion process was calculated using the following equations:[22]

$$S = RT/n^2F^2c\sqrt{2D}; S = 1/Q\sqrt{2} \tag{8}$$

The concentration 'c' of mobile species was calculated by using the formula[23]

$$c = RT/\sigma n^2F^2\sqrt{2D} \tag{9}$$

where the Warburg coefficient σ was calculated by[19]

$$Z'' = \sigma\omega^{-0.5} \tag{10}$$

Diffusion coefficients values were of the order of 10^{-6} cm^2 s^{-1}, where ion movement was high and potential dependent. The concentration of the mobile species (Cu^+) was of the order of 10^{-6} mmol/mL. The inward diffusion of OH^- and outward movement of Cu ions were suggested in this buffer solution because the anodically formed film was a complex function of its formation mechanism, presence or absence of electric field and incorporation of water during preparation.[21] Therefore, transport of Cu^+ ions in the film due to compressive stress generated as a result of applied potential cannot be ruled out as also in passive films on aluminum.[24]

According to point defect model the oxidation of metal atoms to form ions at the metal/oxide (inner) interface generated a driving force to form anion vacancies.[25,26]

$$Cu_{Cu}(m) = Cu_{Cu}(ox) + 1/2V^{\cdot\cdot}{}_o(ox) + e \tag{11}$$

where Cu_{Cu}(m), a copper atom in a regular metal site, $Cu_{Cu}(ox)$, a copper cation in a regular site of the oxide film, $V^{\cdot\cdot}{}_o$, a positively charged oxygen vacancy, and e represented the electron. At the oxide/electrolyte (outer) interface anion vacancies became occupied by anions:

$$V^{\cdot\cdot}{}_o(ox) + H_2O(aq) = O_o(ox) + 2H^+(aq) \tag{12}$$

where $O_o(ox)$ is an oxygen anion in a regular site of the oxide film and $H^+(aq)$ the hydrogen ion in the aqueous electrolyte. Cation vacancies, which were formed by dissolution of cations into the electrolyte, diffused towards the inner interface

$$Cu_{Cu}(ox) = Cu^+(aq) + V'_{Cu}(ox) \tag{13}$$

where these could be exchanged with cations:

$$Cu_{Cu}(m) + V'_{Cu}(m) = Cu_{Cu}(ox) + V_{Cu}(m) + e \tag{14}$$

where $Cu^+(aq)$ is a positively charged copper cation in the aqueous electrolyte, $V'_{Cu}(ox)$ a negatively charged cation vacancy in the oxide, $V'_{Cu}(m)$ a negatively charged vacancy at the metal surface, and $V_{Cu}(m)$ a neutral vacancy in a regular metal site.

$$Cu_{Cu}(ox) = Cu^+_{duplex} + V''_{Cu(ox)} \tag{15}$$

where Cu^+_{duplex} showed the ion that moved into the duplex film and $V''_{Cu(ox)}$, vacancy created in the Cu_2O layer.

The ionic movement started at 0.1 V instead of 0.2 V in comparison to the passive film formed in buffer of pH 9.2.[1]

The interfacial capacitance (Q_1) of the oxide/electrolyte interface slightly decreased upon an increase in potential. However, the surface homogeneity still remained. The Q_1 values are higher than typical capacitance values observed for an oxide covered surface of metal.[1] An increase in R_{por} at 0.1 V and then further to a maximum at 0.3 V suggested that Cu^{1+} ions from the barrier layer diffused and accumulated in the duplex layer (refer to Table). The maximum charge at the oxide/metal interface (Q_2) was at 0.1 V and decreased with the applied potential, thus rendering the film similar to solid solution, as also supported by the low n_2 value.[27]

Final stage

Best fit Nyquist plots in Figure 4 in the 0.4-0.9 V potential range showed a curvature at 0.4 V. At 0.5, this arc transformed into a rising curve, suggesting diffusion of OH^- ions opposite to Cu^{1+} due to increased porosity and at 0.6 V the curve showed competition between diffusion and charge transfer reaction. A skewed semicircle at 0.7 V, which gradually opened up as the potential increased to 0.9 V, indicated that the charge transfer reaction finally superseded the diffusion process. The changes in film texture were apparent as Z' and Z'' varied with potential.

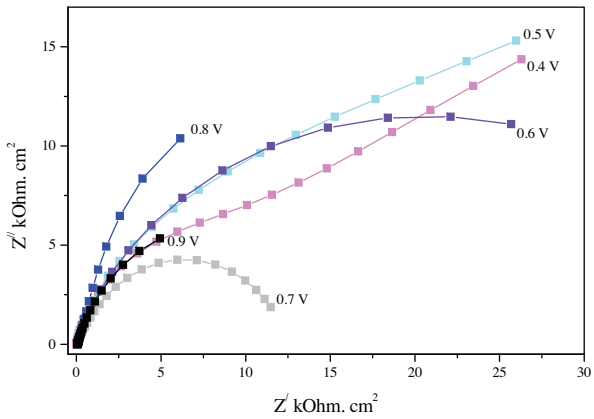

Figure 4. Nyquist plots for the final stage of passivation of copper surface.

The influence of potential change on the oxide/electrolyte and oxide/metal interface was reflected in the best fit parameters for circuit (a) in Figure 2. The growth of the duplex film was accompanied by the formation of CuO, which restarted at 0.4 V after diffusion of Cu^{1+} into the duplex film stopped. The formation of CuO islands from the oxidation of Cu_2O increased the roughness of the surface[28] as also shown by scanning tunneling microscopy (STM).[29] The resistance R_{por} increased and attained a maximum value of 6.67 $k\Omega\ cm^2$ at 0.5 V due to CuO growth from Cu_2O on the electrode surface, which had a smaller molar volume (12.4 $cm^3\ mol^{-1}$) than Cu_2O (23.9 $cm^3\ mol^{-1}$), and thus made the film compact. Initially Q_1 showed a little variation followed by an increase at higher potentials. This showed variation of film texture with pH.[1] At 0.7 V conversion of CuO to $Cu(OH)_2$ through a charge transfer process continuously decreased R_{por} and increased Q_1 and n_1, indicating trapping of charged species, due to dissolution of $Cu(OH)_2$ having molar volume of 29.0 $cm^3\ mol^{-1}$.

The charge transfer process continued at 0.8 V and 0.9 V also causing a further decrease in R_{por} and an increase in Q_1. Dissolution of $Cu(OH)_2$ may also be a factor at these potentials that affected the value of n_1.

The film possessed semiconducting properties[30] and according to the band structure model of semiconductors, the valence band and Fermi level cross above 0.308 V for Cu_2O, thus causing injection of an acceptor level, i.e. Cu^{2+} states that finally lead to the formation of CuO and $Cu(OH)_2$ as potential was further increased to 0.708 V. According to Strehblow any further potential increase would be located at the Cu^{2+} oxide/electrolyte interface.[10] Therefore, it is expected that a potential increase to 0.7 V would give hydroxide of copper according to the reaction[31]

$$CuO + 2OH^- = Cu(OH)_2 + O^{2-} \tag{16}$$

The formation of $Cu(OH)_2$ at higher potential is thermodynamically favorable[15] and also confirmed by the CV results. EIS supports this where Q_2 values together with n_2 values reflected the potential dependence of the film structure.

Variation in Z′ and Z″ at 30 mHz

The Z′ and Z″ values at 30 mHz are plotted in Figure 5. In the initial stage of formation high resistance and low capacitance values indicated the growth of a protective passive film where minimum charge separation could be observed at this interface. This is followed by another peak in the middle region of film formation. The low Z′ value in this region showed structural changes accompanied by slightly increased capacitance values. The lowest values of Z′ are observed in the 0.4 V to 0.9 V potential region, while the maximum charge separation took place at 0.7 V. Imaginary (Z″) and real (Z′) components of impedance have lower values at 0.8 V potential as electrolyte penetrated into the film formed at 0.7 V, leading to increased capacitance and reduced Z′. The 0.9 V potential is peripheral to oxygen evolution potential. It is very likely that some reaction is initiated at this stage that led to decreased capacitance and increased Z′.

Conclusion

The corrosion process strongly depended upon the applied potential. In the first potential stage the film was most stable and its formation and growth over the polycrystalline copper surface followed a consistent pattern in the negative potential regime.

The second stage acted like the demarcation line between the passivation and trans-passivation stages. The diffusion coefficient calculated in conjunction with impedance spectra showed that the film was losing its protective nature with easy ion movement.

In the final potential stage the film structure was severely affected by increasing potential. Therefore, electrolyte supersaturated with Cu^{2+} ions adjacent to metal surface did not cause precipitation of oxides, rather direct oxide growth seems very likely.

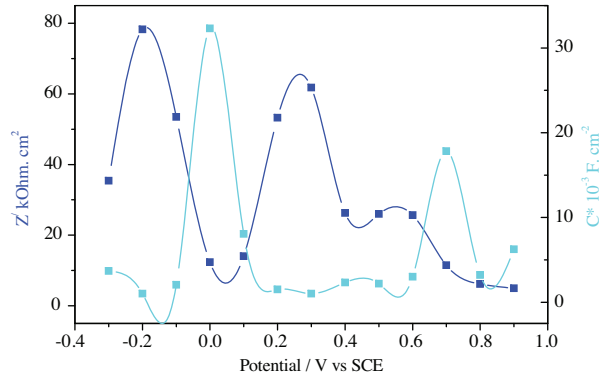

Figure 5. Variation in Z′ and C vs. potential at fixed frequency of 0.03 Hz.

Acknowledgment

We are grateful to Mr. Javed Iqbal helping in the preparation of copper discs, Mr. Bashir-ul-Islam for providing the computer facility, and Ms. Fouzia Altaf for her help during the experimental arrangements.

References

1. Naseer, A.; Khan, A. Y. *Turk. J. Chem.* **2009**, *33*, 739-750.
2. Feng, Y.; Siow, K. S.; Teo, W. K.; Tan, K. L.; Hseih, A. K. *Corrosion* **1997**, *53*, 389-398.
3. Kautek, W.; Gordon II, J. G. *J. Electrochem. Soc.* **1990**, *137*, 2672-2677.
4. Halliday, J. S. *Trans. Faraday Soc.* **1954**, *50*, 171-178.
5. Hickling, A.; Taylor, D. *Trans. Faraday Soc.* **1948**, *44*, 262-268.
6. Dignam, M. J.; Gibbs, D. B. *Can. J. Chem.* **1970**, *48*, 1242-1250.
7. Shoesmith, D. W.; Rummery, T. E.; Owen, D.; Lee, W. *J. Electrochem. Soc.* **1976**, *123*, 790-799.
8. Xia, X.; Xie, C.; Cia, S.; Yang, Z.; Yang, X.; *Corros. Sci.* **2006**, *48*, 3924-3932.
9. Sandberg, J.; Odnevall Wallinder, I.; Leygraf, C.; Le Bozec, N.; *Corros. Sci.* **2006**, *48*, 4316-4338.
10. Strehblow, H.-H.; Collisi, U.; Druska, P. *Proc. International Symposium on Control of Copper Alloys Oxidation*, Rouen, Tranrvied, **1992**, 6.-8. 7.
11. Strehblow, H.-H.; Titze, B. *Electrochim. Acta.* **1980**, *25*, 839-850.
12. Strehblow, H.-H.; Maurice, V.; Marcus, P. *Electrochim. Acta.* **2001**, *46*, 3755-3766.
13. Ambrose, J.; Barradas, R. G.; Shoesmith, D. W. *J. Electroanal. Chem.* **1973**, *47*, 47-64.
14. Droog, J. M. M.; Alderliesten, C. A.; Anderliesten, P. T.; Bootsma G. A. *J. Electroanal. Chem.* **1980,** *111*, 61-70.
15. Pourbaix, M. *Atlas of the Electrochemical Equilibria in Aqueous Solution*; Pergamon Press, New York, 1966.
16. Boukamp, B. A. *EQUIVCRT software manual,* University of Twente Enschede, The Netherlands, 1993.
17. Kramer, M.; Tomkiewicz, M. *J. Electrochem. Soc.* **1984**, *131*, 1283-1288.
18. Lin, H. S. *Phys. Rev. Lett.* **1985**, *55*, 529-532.
19. Walter, G. W. *J. Electroanal. Chem.* **1981**, *118*, 259-273.
20. Fernandes J. C. S.; Ferreira, M. G. S.; Rangel, C. M. *J. Appl. Electrochem.* **1990**, *20*, 874-876.
21. Diggle, J. W.; Downie, T. C.; Goulding, C. W.; Chem. Rev. **1969**, *69*, 365-405.
22. Metikos-Hukovic, M.; Omanovic, S. *J. Electroanal. Chem.* **1998**, *455*, 181-189.
23. Babic, R.; Metikos-Hukovic, M.; *Thin Solid Films* **2000**, *359*, 88-94.
24. Vermilyea, D. A. *J. Electrochem. Soc.* **1963**, *110*, 345-346.
25. Chao, C. Y.; Lin, L. F.; Macdonald, D. D. *J. Electrochem. Soc.* **1981**, *128*, 1187-1194.
26. Macdonald, D. D.; Ben-Haim M.; Pallix, J. *J. Electrochem. Soc.* **1989**, 136, 3269-3273.
27. Tsai, Y. T.; Whitemore, D. H. *Solid State Ionics* **1982**, *7*, 129-139.
28. Collisi Udo; Strehblow, H-H. *J. Electroanal. Chem.* **1990**, *284*, 385-401.
29. Maurice, V.; Strehblow H.-H.; Marcus, P. *J. Electrochem. Soc.* **1999,** *146*, 524-530
30. Babic, R.; Metikos-Hukovic, M.; Jukie, A. *J. Electrochem. Soc.* **2001**, *148*, B146-B151.
31. Lohrengel, M. M.; Schultze, J. W.; Spekmann, H. D.; Strehblow, H.-H. *Electrochim. Acta* **1987**, *32*, 733-742.